Technical Physics, 2024, Vol. 69, No. 8

13

High-gradient aspherization of substrates with thin-film Al/Si coatings

© K.V. Durov, S.M. Mineev, V.N. Polkovnikov, N.I. Chkhalo

Institute of Physics of Microstructures, Russian Academy of Sciences,
A.V. Gaponov-Grekhov Institute of Applied Physics RAS,
603950 Nizhny Novgorod, Russia
e-mail: zevs2801@mail.ru

Received May 15, 2024
Revised May 15, 2024
Accepted May 15, 2024

The paper discusses the issues of film aspherization. A multilayer Al/Si structure has been proposed as an aspherizing coating. It was applied to a spherical surface. By selecting the ratio of materials in the period, a state was searched in which stresses in the multilayer structure were minimized. At the same time, the period of the structure of 9−10 nm corresponds to the mirrors of normal incidence for the wavelength range of 17−19 nm, which are of interest to solar astronomy. Using precision shaped diaphragms, an aspherical coating profile with a maximum height difference of $\sim 1.3\,\mu$m microns was formed between the magnetron and the substrate.

Keywords: thin films, magnetron sputtering, internal stresses, aspherization.

DOI: 10.61011/TP.2024.08.59006.172-24

Introduction

The issues of aberrations and their minimization are of fundamental importance for optical systems of imaging optics. The mirrors of optical circuits should have an aspherical surface shape rather than a spherical one due to the presence of spherical aberrations. The presence of aberrations affects the resolution of the optical device, which includes considered elements. This effect can be illustrated by the example of mirrors for orbiting solar telescopes TEREK (1988) [1], TEREK-K (1994) [2,3], SPIRIT (2001) [4] and TESIS (2009) [5,6].

The TEREK space telescope used spherical mirrors. The angular resolution was 10 arc. sec. (corresponding to a linear resolution over the Sun's disk of about 10 thousand kilometers). The TEREK-K space telescope already uses aspherical toroidal mirrors. The resolution was 5 arc. sec. Aspherization of the mirrors to the shape of a paraboloid of rotation made it possible for the SPIRIT telescope to achieve an angular resolution of 3 arc. sec. and for the TESIS telescope — 1.7 arc. sec. (corresponding to a linear resolution over the Sun's disk of the order of 1 thousand kilometers). Thus, the aspherical shape of the mirrors of imaging optical systems significantly increases the resolution and, one can say, is a necessity.

Only spherical blanks are produced when machining substrates with acceptable accuracy. They can be formed into an aspherical shape in two ways. The first technique involves etching of the surface of a spherical billet with accelerated ion beams [7]. In this case, areas that protrude above the desired profile are removed from the surface of the optical element. The second approach is the vacuum deposition of a thin-film coating. It was used, for example, to create aspherical mirrors of the SOHO solar telescope [8].

Each of these methods has advantages and disadvantages. For instance, the ion beam etching forms a blank without application of additional materials to its surface. Such a substrate can then be subjected to chemical treatment (for example, to clean the surface of dirt) no risk of destruction or damage to the aspherizing coating. At the same time, there are a number of materials (for example, beryllium) whose surface cannot be treated with ion beams without development of roughness [9]. Then the natural solution is to apply the film aspherization technique.

This raises the question of choosing aspherizing coating materials. They should, first, have good adhesion to the substrate material to prevent the coating from peeling off from the substrate. Second, aspherizing films should maintain a low surface roughness. The latter requirement is associated with the need to subsequently apply a multi-layer reflective coating to the substrate. The roughness of the substrate and the reflective coating should have low values of no more than a few angstroms to ensure high X-ray reflection coefficients.

An aspherizing boron-based coating was proposed in Ref. [8]. Its thickness was 350 nm. It was also noted that when the boron film exceeds the thickness of 300 nm, it begins to peel off from the substrate. The authors applied an additional layer of tungsten for better adhesion of the boron film to the substrate.

A multi-layer aspherizing coating based on Mo/Si [10] was proposed for the mirrors of the SPIRIT telescope. Since the reflective coating was also a Mo/Si multi-layered structure (MLS), but with a different period, this resulted in a simplification of the technological process. The thickness of the aspherizing film was about 300 nm.

However, the Mo/Si MLS used in this case has a number of significant drawbacks. Firstly, unaccounted for internal coating stresses which are quite significant reaching several hundred MPa as shown in Ref. [11], will inevitably lead to distortion of the final shape of the mirror surface. It is estimated that the deformation of the substrate in this case can reach 20−30 nm. These values significantly exceed the Marechal criterion for diffraction quality optics: shape deviations from a given surface of not more than $\lambda/14$. $\lambda = 2{-}30$ nm in the case of optics in the X-ray and vacuum ultraviolet wavelength ranges. Stress-free (with zero internal stresses) state of the Mo/Si film is possible only at a significant thickness of molybdenum, which is accompanied by the development of roughness [12]. Secondly, there is no selective chemical etchant for Mo/Si that does not simultaneously destroy the surface of a quartz or silicon substrate. Thus, it is not possible to restore the substrate in the event of an unsuccessful synthesis process (remove deposited materials from it without consequences for the optical surface).

The authors replaced the Mo/Si MLS with an alternative Cr/Sc structure. They selected the ratio of Cr and Sc, which provides compensation for internal reflections. The substrate roughness did not develop with the deposited film. In addition, Cr/Sc dissolves in a weak solution of hydrochloric acid without any consequences for the quartz or silicon surface, i.e. an aspherizing coating based on Cr/Sc simultaneously acts as a sacrificial layer when it is necessary to restore the substrate. The total range (difference between maximum and minimum) of the aspherizing film heights was 130 nm.

The film thickness was at the level of $0.1{-}0.3\,\mu$m in all film aspherization examples described above. We studied materials for higher gradient aspherization (with a height difference of more than $1\,\mu$m) in this paper. The following requirements were applied to all of them:

a) maintaining a low surface roughness;

b) stress-free state;

c) high film growth rate.

Al/Si MLS is proposed as the basis for aspherizing coating. First, the aluminum sputtering coefficient, and hence the film growth rate, is high. Secondly, it is known from previous studies in Ref. [13] that the Al/Si MLS has a low interlayer roughness (at the level of 0.6 nm), i.e., it is possible to expect a corresponding surface roughness.

Another important advantage of the Al/Si MLS over other aspherizing coating compositions is the possibility of using it as a reflective coating for the wavelength range 17−19 nm, i.e. it will be possible to limit the use of two magnetron sources such as with aluminum and silicon targets when fabricating aspherical mirrors optimized for this range.

Internal stresses in Al/Si films have not been studied before.

Figure 1 shows the calculated dependence of the film coating thickness on the radial coordinate of a substrate with a diameter of 110 mm.

The maximum film thickness $D = 1332$ nm is 38 mm from the center of the substrate. The thickness decreases to 422 nm at the edge of the central hole. The thickness drops

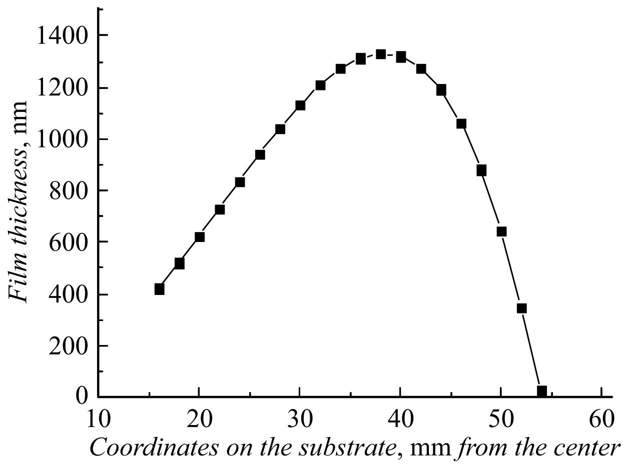

Figure 1. Experimental distribution of the thickness of the aspherizing coating as a function of the radial coordinate of the substrate.

to 24 nm at the edge of the substrate. This is a significant gradient. Such values have not yet been achieved in practice.

1. Experimental method

Film aspherization is achieved by depositing a thin film with a thickness variable over the substrate area on the substrate surface. Deposition methods, generally speaking, can be different. The magnetron sputtering method is the simplest method in terms of precise control of the thickness distribution. At the same time, it is poorly suited for sputtering dielectric materials because the direct current sputtering of such targets is impossible in principle, and sputtering in a high-frequency discharge has low film growth rates. Accordingly, these rates make it difficult to obtain coatings with large (in units-tens of micrometers) thicknesses and, accordingly, thickness differences. Sputtering of dielectric targets with a neutralized ion beam can be considered as an alternative to high-frequency discharge.

The above methods were combined in the magnetron and ion-beam sputtering system for multilayer structures designed and created by IPM RAS [14].

The working chamber is a cylindrical volume with a height of 500 mm and a diameter of 800 mm. Magnetron sources are evenly distributed along the perimeter of the bottom of the working chamber. They are sources of the planar type. The magnetic field of the arched configuration contributes to the formation of an annular erosion zone on the target surfaces (the inner diameter of the ring is 95 mm, the outer diameter is 115 mm). This configuration allows for simple application of coating on substrates with a diameter of up to 120 mm with an uniform or predetermined distribution and the coatings can be applied on substrates with the diameter of up to 200 mm with the use of a number of process techniques.

Magnetron power sources are stabilized DC units developed by IPM RAS. They allow varying the discharge current within 100–2000 mA at voltages from 100 to 500 V. „Balzers“ units with a frequency of 13.56 MHz are used for high-frequency sputtering of targets. Typical values of electrical power are in the range of 150–250 W in the synthesis process.

Figure 2 shows the installation diagram For a better understanding of the technological process (without ion sources, since only magnetron sputtering was used in the work).

The substrate is mounted with the working surface facing down on a rotating disk located above the magnetrons. When the disk rotates, the substrate passes over the working magnetrons. This allows applying layers sequentially one after the other. A full period of the structure is sputtered out in one complete rotation of the disk. By changing the speed of the substrate passage (the angular velocity of disk rotation) over the magnetrons, it is possible to adjust both the ratio of layer thicknesses in the period and the value of the period itself.

The characteristic film growth rates for magnetron sputtering at direct current are 0.1–1 nm/s, depending on the target material and on the electrical power applied to it. These rates are 5–10 times lower for a high-frequency discharge. The growth rates of Si and Al films were ~ 0.14 and 0.55 nm/s, respectively, in our experiments.

The cycle of work for creating a multi-layer coating includes a procedure for ensuring the necessary distribution of the thickness of the layers of sprayed materials over the substrate area. Shaped precision diaphragms are located above each magnetron to ensure either uniformity or a given distribution of the coating over the substrate area. By changing their shape, it is possible to control the distribution of the flux density of the substance entering the substrate. The accuracy of controlling the period distribution over the mirror area is of the order of 0.5% of the period value.

Such shaped diaphragms were used for aspherization of films of the mirrors of the SPIRIT and TESIS solar observatories. It is important to note that the technology

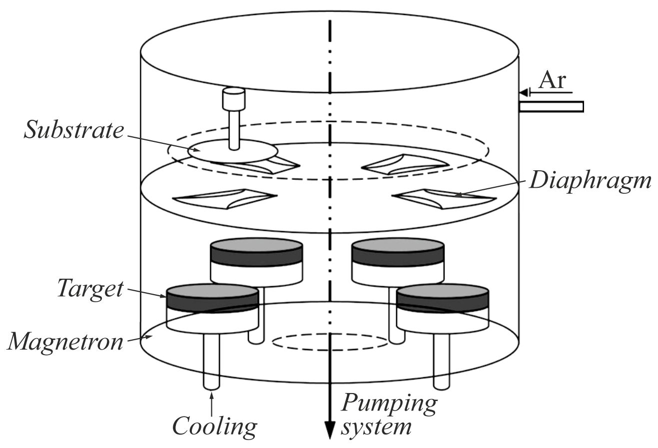

Figure 2. Magnetron sputtering installation diagram.

allows ensuring differences with a large range of heights. The thickness of the coating over the substrate area can vary by an order of magnitude at distances of tens of millimeters. It is difficult to ensure such a sharp height difference within units of millimeters by other methods.

The procedure for creating a given material thickness distribution is iterative. At the first stage, MLS is deposited on super-smooth silicon wafers fixed on a metal surface with a radius of curvature equal to that of the working substrate. After sputtering, small-angle X-ray diffraction measurements are performed on a Philips X'Pert PRO diffractometer (Philips Analytical, the Netherlands). Measurements and subsequent processing of the results of small-angle X-ray diffraction using the program „Multifitting“ [15] allows determining most of the MLS parameters (period, individual material thicknesses in the period, roughness, etc.). The obtained real thickness distribution over the substrate area is compared with the calculated one. If necessary, the shape of the precision diaphragms is corrected and re-sprayed with subsequent measurements. The final stage involves sputtering of the „working“ structure onto the „working“ substrate.

It is important that the aspherizing coating has a minimum value of internal stresses s (stress). It is necessary to adhere to the generally accepted terminology for unambiguity. Stresses in a film (solid or multi-layered) can be tensile, when the film seems to try to contract on the substrate — the force counteracts compression, „stretches“ film and is directed from the center of the substrate to the periphery. In this case, it is customary to assign the sign „plus“ to s. Stresses can also have a compressive character when forces are directed from the periphery to the center. Then it is customary to talk about negative stresses and assign „minus“ to s. The film + substrate system has a concave character with the sign „plus“ it has a convex character with the sign „minus“ with the film curved outwards.

The most obvious methods for measuring stresses are based on the following property. The substrate will bend if the film is deposited in a stressed state on the surface of the substrate. This bending can be measured, and the corresponding stress is calculated from the results of measuring the curvature of the system using the Stoney formula [16]:

$$s = \frac{E}{6(1-\nu)} \frac{d_{\text{substr}}^2}{d_{\text{film}}} \left(\frac{1}{R_{\text{after}}} - \frac{1}{R_{\text{before}}} \right), \tag{1}$$

where E and ν is the Young's modulus and Poisson's ratio of the substrate material, d_{substr} and d_{film} is the substrate and film thicknesses, R_{before} and R_{after} are the radii of curvature of the substrate before and after film deposition.

Otherwise, the methods differ only in the approaches to determining the radius of curvature of the substrate. For an overview of these methods, see [17]. The radii of curvature of the substrates in our experiments and consequently the internal stresses were determined using

Characteristics of multilayer Al/Si structures

d, nm	β(Si), rel.u.	s, MPa	σ_{eff}, nm	σ_{Al}, nm	σ_{Si}, nm
10.54	0.68	-417	0.84	0.62	0.74
10.06	0.50	-322	0.83	0.70	0.76
9.33	0.42	-174	0.82	0.90	0.91
8.74	0.30	-84	0.81	0.95	0.93
8.70	0.20	-39	0.80	0.97	0.96
8.96	0.15	-67	–	–	–

VerifireTM 4 interferometer using the method described in Ref. [18]. The radius of curvature of the substrate was determined by comparing the profile of the substrate before and after applying the reflective coating with the profile of the reference surface embedded in the interferometer. Measurement on an interferometer allows determining the deviation of the profile of the measured substrate from the profile of the reference. The transmission reference plane acts as a reference, the size is about 100 mm, the reflection coefficient is 4%, the shape accuracy is better than $\lambda/20$, $\lambda = 555$ nm. The stated absolute error of determining the profile using this device is 10 nm.

Surface roughness was estimated using a specialized test bench based on atomic force microscope Ntegra (NT-MDT) [19].

The shape of the substrate surface after the film asopherization procedure was studied using an interferometer with a diffraction comparison wave [20], built on the basis of a unique reference spherical wave source — narrowed to sub-wave dimensions of an optical fiber.

2. Results and their discussion

Before proceeding to the procedure of forming an asopherization profile, it is necessary to determine the optimal parameters of the structure from the point of view of internal stresses. More precisely — the ratio of materials in the period. A number of Al/Si structures with 40 periods were synthesized for this purpose. MLS differed in the ratio of materials in the period. On average, the selected structure periods are about 9–10 nm. These values correspond to multilayer normal-incidence mirrors for the spectral range of 17–19 nm.

This range is of interest for problems of solar astronomy. The lines of radiation of FeIX-FeXII ions formed at a plasma temperature of 1.3–1.6 MK fall within this range. Multilayer mirrors based on Al/Si in the considered spectral range have a high spectral selectivity of $\Delta\lambda = 0.4$ nm [13]. This property makes them promising for solving spectroscopic problems of solar physics. Since solar telescopes belong to imaging systems, it becomes very important to take into account internal stresses that lead to elastic deformations of substrates, so the results of our study are important not only for asopherization problems, but also for creating solar telescopes focused on the spectral range 17–19 nm.

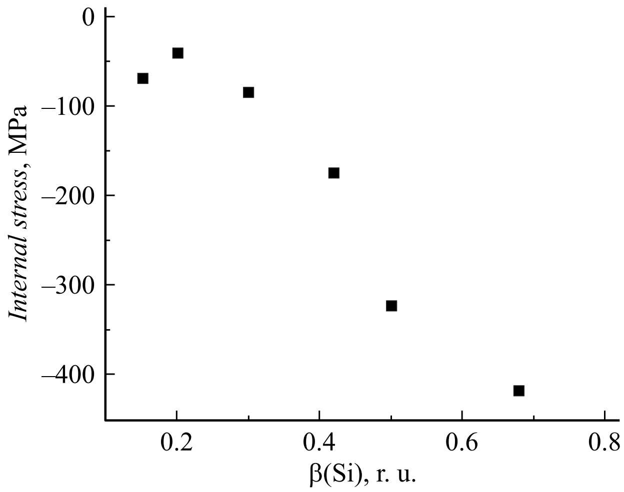

Figure 3. Dependence of internal stresses in multilayer Al/Si films on the value $\beta = d(\text{Si})/d$.

The following table shows the results of a series of experiments with MLS having a different ratio of materials in the period. Here d — period of the structure, $\beta = d(\text{Si})/d$ — fraction of the silicon layer in the period, s — internal stresses in the film, σ_{eff} — surface roughness, σ_{Al} — interlayer roughness at the Si-on-Al interface, σ_{Si} — interlayer roughness at the Al-on-Si interface.

Figure 3 graphically shows the dependence of internal stresses on the value β for greater ease of perception.

Internal stresses of the Al/Si MLS are compressive. A close to linear relationship is observed in the range of β values from 0.20 to 0.68. It is possible to expect that the value of s will be close to zero at $\beta = 0.15$, but in practice an inflection and an increase of compressive stresses is observed. The lowest value of $s = -39$ MPa is observed at $\beta = 0.20$.

It is interesting to note that the maximum reflectivity of the Al/Si MLS falls on the value $\beta = 0.50$ according to the data provided in Ref. [13]. $s = -322$ MPa is a rather significant value in this case that can lead to significant elastic deformations in accordance with Fig.3 and the table. This circumstance should be taken into account when fabricating mirrors for solar telescopes. The method of deposition of „anti-stress“ multilayer coating can be applied for compensating deformations caused by Al/Si MLS. It should have a tensile character of internal stresses. A Cr/Y film with a higher proportion of chromium in the period may be suitable as such an MLS [13].

Let us suppose that we need to compensate for deformations caused by an Al/Si mirror with a value $s = -322$ MPa, a period of 9 nm, and a number of periods 60 (the total coating thickness is 540 nm). It is possible to use the Cr/Y structure with the chromium thickness in the period of 3.3 nm, and scandium thickness in the period of 2 nm in accordance with the data provided in Ref. [13]. In this case,

$s = +600$ MPa. 55 periods of such a Cr/Y MLS will be required for compensation.

It is noteworthy that the sub-nanometer value of the surface roughness is at the level of 0.8 nm for all studied samples. The difference from this value of interlayer roughness (from 0.6 to 0.9 nm) can be explained by its corresponding character as the interlayer roughness consists of geometric roughness and mixing of materials at the interfaces. It is possible to conclude based on the above dependences that it is mixing that increases with a decrease of β, and the geometric roughness remains approximately at the same level.

It is important to note that a certain increase of surface roughness takes place in the case of a noticeable increase of the number of periods (to achieve a given value of aspherizing coating). In particular, the value of $\sigma_{\text{eff}} = 1.5$ nm was observed in the experiment for a structure with $\beta = 0.30$ and 300 periods, while the interlayer roughness remains at 0.9 nm. However, the reflection coefficient at a wavelength of 17.7 nm will decrease from 40 to 24% if an Al/Si mirror with a period of 9 nm is applied to a surface with a roughness of not 0.8, but 1.5 nm.

It follows from the above dependences that the minimum value of internal stresses has a structure with the value of $\beta = 0.20$. This composition was chosen for the creation of the aspherizing coating.

Since the synthesis of a full-fledged film with a maximum thickness of the order of $1.3\,\mu$m takes up to two full working days, the profile of the aspherizing coating was derived with structures of much smaller thickness (with a number of periods of 30 and a total thickness of about 300 nm). To compare the obtained values of the film thickness distribution with a given profile, they (coating thicknesses and a given profile) were normalized by one and compared on one graph. An example of such a comparison is shown in Fig. 4.

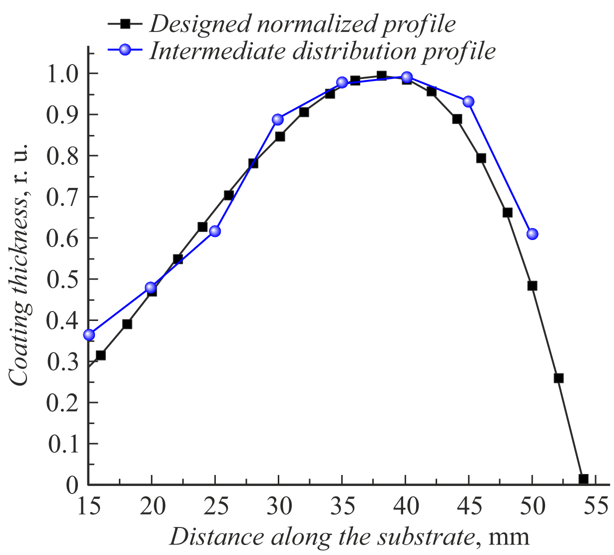

Figure 4. Example of comparison of the thickness of an aspherizing coating and a given profile.

The deviation of the obtained distribution profile from the specified one was analyzed based on these data. The precision orifices expand at the point where the resulting profile goes below the specified one, and vice versa. As a result, a configuration of precision diaphragms was obtained, ensuring a thin-film coating profile close to the specified one.

At the final stage, an Al/Si multilayer structure with a number of periods $N = 160$ was deposited on a concave spherical substrate with a diameter of 108 mm and a surface radius of curvature of $R = 266.6$ mm, ensuring a maximum coating thickness of 1332 nm.

Figure 5 shows the initial (before aspherization) profile of the surface deviation from the sphere (a) and the resulting (after aspherization) profile (b).

The exact value of the height span is $1.566\,\mu$m according to the map in Fig. 5, b. It should be noted that the deviation of the initial profile from the sphere was about $0.24\,\mu$m without taking into account small edge areas. Thus, it was possible to obtain a surface profile close to the specified one.

Conclusion

Multilayer Al/Si films with a period of about 9–10 nm and a different ratio of material thicknesses in the period were examined in the result of the studies. The values of internal stresses were determined. It was demonstrated that the lowest value of −39 MPa is achieved with the silicon layer share in the period of 0.20. The internal stresses will be about −300 MPa for a structure with parameters optimized for maximum reflectance in the spectral range 17–19 nm.

The values of surface and interlayer roughness were determined. They are important to keep in mind for the subsequent deposition of a reflective coating on the surface of the aspherizing film. The surface roughness of the Al/Si structure with 40 periods is about 0.8 nm, while the surface roughness of the structure with 300 periods increases to 1.5 nm.

A method of film aspherization using an Al/Si MLS with a minimum value of internal stresses and with a height range up to $1.3\,\mu$m was developed.

Funding

Synthesis and film aspherization was supported by the Russian Science Foundation grant 21-72-30029, and the study of internal stresses was carried out within the scope of the State Assignment FFUF-2024-0022.

Conflict of interest

The authors declare that they have no conflict of interest.

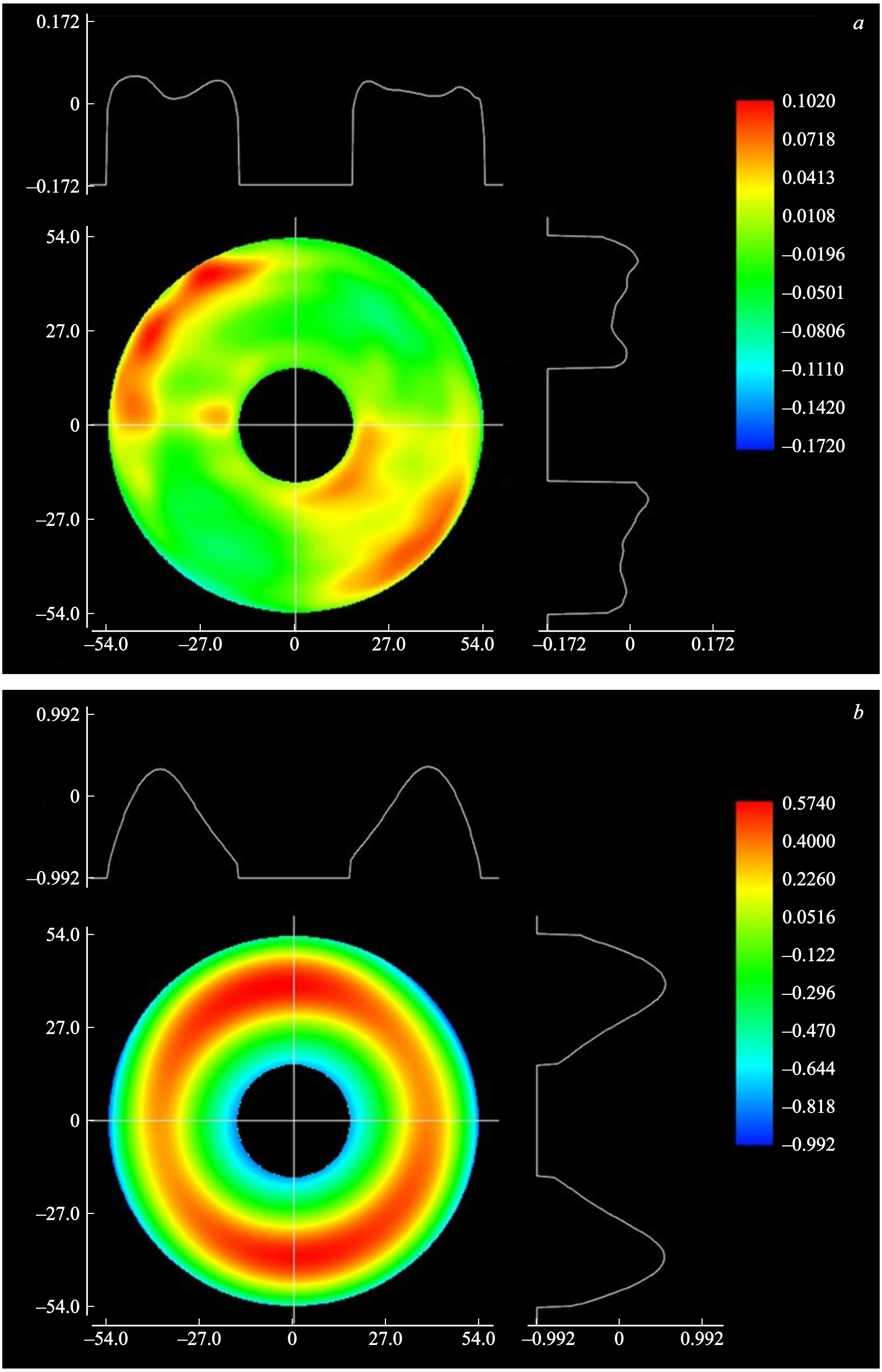

Figure 5. Map of substrate surface heights before (*a*) and after (*b*) aspherization.

References

[1] I.I. Sobelman, I.A. Zhitnik, B. Valnichek, M. Rybanski, M. Bernas, S.V. Gaponov, R. Gudets, A.P. Ignatiev, R.V. Isadzhanyan, V.M. Kishchenko, M. Klima, Ya. Kopetski, V.V. Korneev, O.B. Krasnopolsky, M.N. Krmoyan, V.V. Krutov, V.M. Lomkova, A.V. Mitrofanov, S.N. Oparin, R. Persty, A.A. Pertsov, N.N. Salashchenko, V.A. Slemzin, A.B. Telegin, V.O. Timofeev, I.P. Tindo, A.M. Urnov, Yu.N. Fotin, Yu.M. Khojayants. Pisma v AZh, **16** (4), 323 (1990) (in Russian).

[2] I.I. Sobelman, I.A. Zhitnik, A.P. Ignatiev, V.V. Korneev, V.Yu. Klepikov, V.V. Krutov, S.V. Kuzin, A.V. Mitrofanov, S.N. Oparin, A.A. Pertsov, N.N. Salashchenko, V.A. Slemzin, A.I. Stepanov, I.P. Tindo, E.A. Avetisyan, V.M. Lomkova, V.F. Sukhanov, Yu.N. Fotin. Pisma v AZh, **22** (8), 604 (1996) (in Russian).

[3] I.A. Zhitnik, A.P. Ignatiev, V.V. Korneev, V.V. Krutov, S.V. Kuzin, A.V. Mitrofanov, S. Oparin, A.A. Pertzov, V.A. Slemzin, I.P. Tindo, M. Pakhomov, N.N. Salashchenko, O. Timofeev. Proc. SPIE, **3406**, 1 (1998).

[4] B.N. Oraevsky, I.I. Sobelman. Pisma v AZh, **28** (6), 34 (2002) (in Russian).

[5] S.V. Kuzin, I.A. Zhitnik, O.I. Bugaenko, A.P. Ignatiev, A.V. Mitrofanov, S.N. Oparin, A.A. Pertsov. Izvestiya RAN. Ser. fiz., **69** (2), 191 (2005) (in Russian).

[6] O.I. Bugaenko, S.V. Kuzin, S.A. Bogachev, I.A. Zhitnik, A.A. Perzov, A.P. Ignatiev, A.M. Mitrofanov, V.A. Slemzin, S.V. Shestov, N.K. Sukhodrev. Adv. Space Res., **43** (6), 1001 (2009).

[7] I.V. Malyshev, D.G. Reunov, N.I. Chkhalo, M.N. Toropov, A.E. Pestov, V.N. Polkovnikov, N.N. Tsybin, A.Ya. Lopatin, A.K. Chernyshev, M.S. Mikhailenko, R.M. Smertin, R.S. Pleshkov, O.M. Shirokova. Optics Express, **30** (26), 47567 (2022).

[8] J.-P. Delaboudiniere, R.A. Stern, A. Maucherat, F. Portier-Fozzani, W.M. Neupert, J.B. Gurman, R.C. Catura, J.R. Lemen, L. Shing, G.E. Artzner, J. Brunaud, A.H. Gabriel, D.J. Michels, J.D. Moses, B. Au, K.P. Dere, R.A. Howard, R. Kreplin, J.M. Defise, C. Jamar, P. Rochus, J.P. Chauvineau, J.P. Marioge, F. Clette, P. Cugnon, E.L. van Dessel. Adv. Space Res., **20** (12), 2231 (1997).

[9] N.I. Chkhalo, M.S. Mikhailenko, A.E. Pestov, V.N. Polkovnikov, M.V. Zorina, S.Yu. Zuev, D.S. Kazakov, A.V. Milkov, I.L. Strulya, V.A. Filichkina, A.S. Kozlov. Appl. Opt., **58**, 3652 (2019).

[10] S.S. Andreev, S.Yu. Zuev, V.I. Pozdnyakova, N.N. Salashchenko, V.A. Slemzin, I.L. Strulya, I.A. Shereshevsky, I.A. Zhitnik. Poverkhnost. Rentgenovskie, sinkhrotronnye i neytronnye issledovaniya **1**, 6 (2003) (in Russian).

[11] S.S. Andreev, E.B. Klyuenkov, A.L. Mizinov, V.N. Polkovnikov, N.N. Salashchenko, L.A. Suslov, V.V. Chernov. Poverkhnost. Rentgenovskie, sinkhrotronnye i neytronnye issledovaniya **2**, 45 (2005) (in Russian).

[12] S.S. Andreev, S.V. Gaponov, S.A. Gusev, S.Yu. Zuev, E.B. Klyuenkov, K.A. Prokhorov, N.I. Polushkin, E.N. Sadova, N.N. Salashchenko, L.A. Suslov, M.N. Haidl. Poverkhnost. Rentgenovskie, sinkhrotronnye i neytronnye issledovaniya **1**, 66 (2001) (in Russian).

[13] S.A. Bogachev, N.I. Chkhalo, S.V. Kuzin, D.E. Pariev, V.N. Polkovnikov, N.N. Salashchenko, S.V. Shestov, S.Y. Zuev. Appl. Opt., **55** (9), 2126 (2016).

[14] I.G. Zabrodin, B.A. Zakalov, I.A. Kaskov, E.B. Klyuenkov, V.N. Polkovnikov, N.N. Salashchenko, S.D. Starikov, L.A. Suslov. Poverkhnost. Rentgenovskie, sinkhrotronnye i neytronnye issledovaniya, (in Russian). **7**, 37 (2013).

[15] M. Svechnikov. J. Appl. Crystallogr., **53** (1), 253 (2020).

[16] A. Brenner, S. Senderoff. J. Res. Nat'l. Bur. Stand, **42**, 105 (1949).

[17] l. Maissel, R. Glang. *Tekhnologiya tonkih plenok. Spravochnik* (Sovetskoe radio, M., 1977) (in Russian).

[18] R.M. Smertin. Thin Solid Films, **782** (1), 140044 (2023).

[19] N.I. Chkhalo, N.N. Salashchenko, M.V. Zorina. Review Scientific Instruments, **86**, 016102 (2015).

[20] A.A. Akhsakhalyan, N.I. Chkhalo, N. Kumar, I.V. Malyshev, A.E. Pestov, N.N. Salashchenko, M.N. Toropov, B.A. Ulasevich, S.V. Kuzin. Precision Eng., **71**, 330 (2021).

Translated by A.Akhtyamov